Analysis of ILRS data from STPSat-2 Retro-reflector

September 2014

Richard E. Preston, Robert W. Crow (Sensing Strategies, Inc)
Elizabeth A. Beecher (AFRL)
Linda M. Thomas (NRL)

1.0 Summary

This paper presents an evaluation of the scientific utility of a small (1/2 inch diameter), commercial low-cost hollow retro-reflector (RR) used on the STPSAT-2 satellite flown by the USAF Space Test Program (STP). Experiments were carried out over a six-month period and measured returns from four different International Laser Ranging Service (ILRS) sites were reported. The data showed that the RR's angular response fall-off was the limiting factor in obtaining returns. This suggests that the devices are useful for ILRS ranging, but this size would have greater utility on satellites that could be pointed at ILRS test sites on the ground. It is concluded that the RRs would have excellent utility if used on small, inexpensive satellites (e.g., cubesats) with pointing capability which could be widely deployed, thereby increasing the number of satellites available for ILRS and geodesy testing.

2.0 Background

The STPSAT-2 satellite was launched in November 2010.   STPSAT-2 is in a circular orbit at an altitude of 650 km with an inclination angle of 72 degrees. The STP office included a small, hollow RR on the satellite to allow for the possibility of laser ranging experiments.   AFRL and NRL approached NASA about including the STPSAT-2 satellite on the ILRS target list to facilitate an evaluation of the RR and whether the devices might have utility for smaller, cubesat-size geodesy satellites. NASA submitted an ILRS support request and a six-month period of satellite illuminations was planned. For all of the measurements, the STPSAT-2 satellite was in a nominally NADIR facing geometry. The data shown in this report was collected in April-August 2013 time frame.

3.0 Technical Approach

The experimental approach taken for this effort was to characterize the effectiveness of the retro-reflector with ILRS tracking experiments and to interpret those results in light of laboratory cross section measurements. In particular, it was expected that the geometries suitable for detecting returns from the RR would be limited by its angular response which was designed to be close to zero at 30 degrees off the RR centerline.

3.1 Retro-Reflector Description and Expected Utility

The hollow retro-reflector, shown in Figure 1, is a PLX Omni Wave which has a ½ inch diameter, 5 arc second beam deviation and is silver coated with a reflectivity of 0.98 at 1064 nm and 0.96 at 532 nm. The device was mounted on the STPSAT-2 satellite NADIR face.

Figure 1. STPSAT-2 Retro-Reflector

Following Degnan[1], the retro-reflector's predicted cross section, σ_{RR} is computed by multiplying the reflectivity of the device, ρ, by the aperture area of the retroreflector, A_{RR}, and dividing by the diffraction-limited steradiancy of the return beam, Ω, as shown in Equation 1:

$$\sigma_{RR} = \rho \cdot A_{RR} \cdot \frac{4\pi}{\Omega} \ \text{m}^2/\text{sr} \qquad\qquad \text{Equation 1}$$

where

$$\boldsymbol{\Omega = \frac{\pi}{4} \cdot \left(2.44 \cdot \frac{\lambda}{D_{RR}}\right)^2 \ \text{sr}}$$

Equation 2

and D_{RR} is aperture diameter and λ is the laser wavelength, or, simplifying

$$\boldsymbol{\sigma_{RR} = \frac{4\pi \cdot \rho \cdot D_{RR}^4}{(2.44 \cdot \lambda)^2}} \ \text{m}^2/\text{sr} \qquad\qquad \text{Equation 3}$$

Given the RR's 1.27 cm diameter and 0.97 reflectivity at 532 nm, one calculates the expected cross section at 532 nm wavelength to be:

$$\boldsymbol{\sigma_{RR} = 1.88 \cdot 10^5} \ \text{m}^2/\text{sr}. \qquad\qquad \text{Equation 4}$$

It is instructive to compute the expected return signal strength from a RR of this cross section using a laser with parameters representative of those used by the ILRS[2].

$$n_p(\text{electrons}) = \frac{P \cdot \tau_{atm}^2}{\pi/4 \cdot (R \cdot \theta_L)^2} \cdot \frac{\sigma_{RR}}{4\pi \cdot R^2} \cdot \frac{A_o \cdot \tau_L \cdot qe}{h\nu} \qquad\qquad \text{Equation 5}$$

where :

        P is the energy per pulse of the laser transmitted to the satellite,
        T_{atm} is the atmospheric transmission from the ground to the satellite,
        R is the range to the satellite
        θ_L is the divergence of the laser
        A_o is the area of the receiver collecting optic
        τ_L is the optical path transmission of the receiver
        qe is the detector quantum efficiency, and

[1] A Tutorial on Retroreflectors and Arrays for SLR, John J. Degnan, Sigma Space Corporation, ILRS Workshop, Frascati, Italy, November 5, 2012.
[2] Millimeter Accuracy Satellite Laser Ranging: A Review, John J. Degnan, Code 920.1/Space Geodesy and Altimetry Projects Office, NASA/Goddard Space Flight Center, Greenbelt, MD 20771 USA

hv is the energy per photon.

Given a 0.1 J/pulse laser with a 30 arc second divergence, a 700 km range to the satellite, atmospheric transmission (one way) of 70%, a receiver diameter of 0.75 m, an optics transmission of 70% and a qe of 20%, one computes:

$$n_p(\text{elec}) = \frac{0.1J \times .7^2}{\frac{\pi}{4} \cdot (7 \times 10^7 \text{cm} \times 1.45 \times 10^{-4}\text{rad})^2} \cdot \frac{1.88 \times 10^9 \frac{\text{cm}^2}{\text{sr}}}{4\pi(7 \times 10^7 \text{cm})^2} \cdot \frac{4415\text{cm}^2 \times .7 \times .2}{3.71 \times 10^{-19} \frac{J}{\text{ph}}} \approx 31{,}000$$

<div align="right">Equation 6</div>

For detector systems working near a photon counting limit, a burst of 31,000 electrons is a very significant signal indicating that even this small RR in a low earth orbit should have excellent utility for ILRS-class systems. There are two primary concerns that could limit the utility of the RR for these kinds of experiments: the velocity aberration induced by the spacecraft movement and the fall-off in response of the RR as a function of incidence angle. Each of these issues are discussed briefly below.

The velocity aberration[3] is a result of the spacecraft motion relative to the ground site and it produces an angular deflection of the return beam in the direction of the satellite motion given by

$$\alpha \ (rad) = \ 2 \cdot \frac{V}{c} \qquad\qquad\qquad \text{Equation 7}$$

Where V is the velocity of the spacecraft, c is the speed of light and α is the angular displacement. The STPSAT2 spacecraft has a velocity of approximately 7.5 km/sec so it produces a velocity aberration of 50 microradians. Given the 1.27 cm diameter and 532 nm laser wavelength one expects a diffraction limited return beam with the first Airy disk null at 51 microradians (half-angle) which means the direct return beam will be significantly attenuated due to the velocity aberration. It should be noted that at a wavelength of 1.06 microns, the return beam divergence is double the size of the velocity aberration which resolves any experimental concerns.

The return beam from the RR was characterized in laboratory measurements using the set-up shown in Figure 2. The return beam was collected using a beam splitter and a 1 meter focal length lens focused the beam to a profiler camera to measure the spot size and amplitude distribution. Using the relationship

$$div(\text{rad}) = \frac{d}{f} \qquad\qquad\qquad \text{Equation 8}$$

where *div* is the beam divergence, *d* is the spot diameter and *f* is the focal length of the focusing lens.

---

[3] Millimeter Accuracy Satellite Laser Ranging: A Review, JOHN J. DEGNAN, Code 920.1/Space Geodesy and Altimetry Projects Office, NASA/Goddard Space Flight Center, Greenbelt, MD 20771 USA
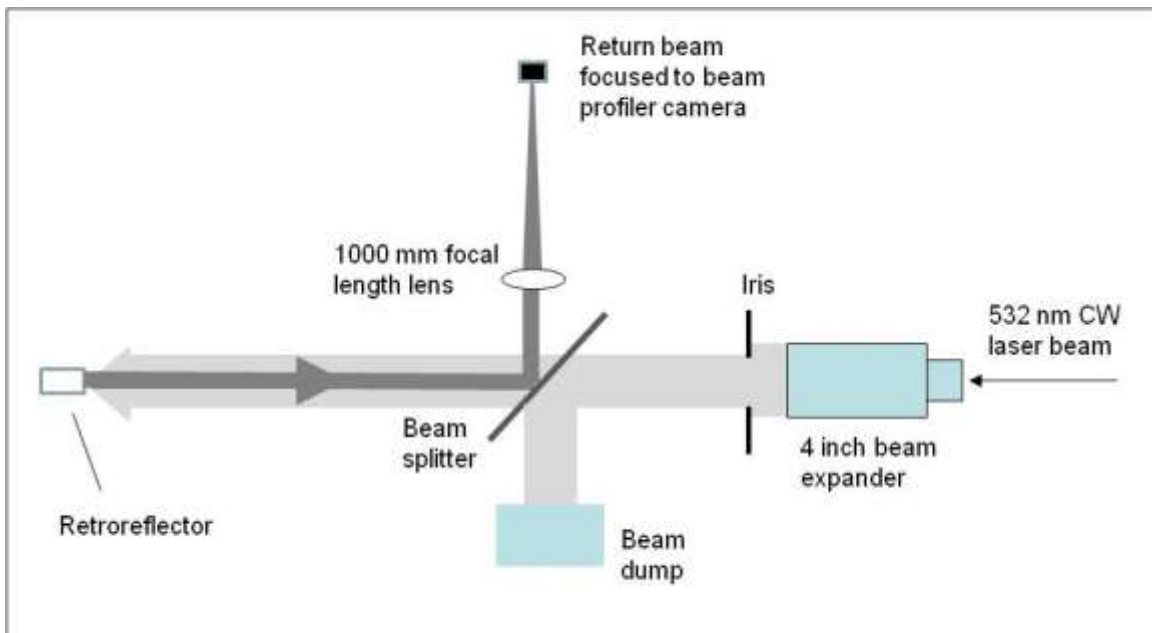
Figure 2 Experimental Set-Up for Return Beam Divergence Measurement

The measured profile for return beam when the RR is orthogonal to the beam is shown in the left-hand panel of Figure 3. The divergence of the on-axis return beam is approximately 53 microradians (µr) or just slightly large than the diffract limit (51 µr The amplitude of the return at 50 µr off-center drops to roughly 1% of the peak value, so given the strong return predicted above, it is reasonable to expect that returns will be detected despite the attenuation due to the velocity aberration. The right-hand panel of Figure 3 shows the return beam profile when the RR is at an oblique angle as is more typically the case in engagement geometries. Since the RR is always NADIR pointing, the cross section for non-overhead geometries becomes elliptical and the return beam spreads in angle as shown in the data. For a 20 degree incidence angle, the return beam divergence was measured (half angle) to be 122 and 68 µr in the long and short axes, respectively. The longer axis will overlap the laser site if the satellite is heading towards or away from the site and the shorter axis will overlap if the satellite path is tangential. In either case, the larger return beam compensates to some extent for the velocity aberration and improves the chances of getting return signals. Measurements at 1.06 microns verified that the RR produced diffraction limited beams as well at that wavelength.

4
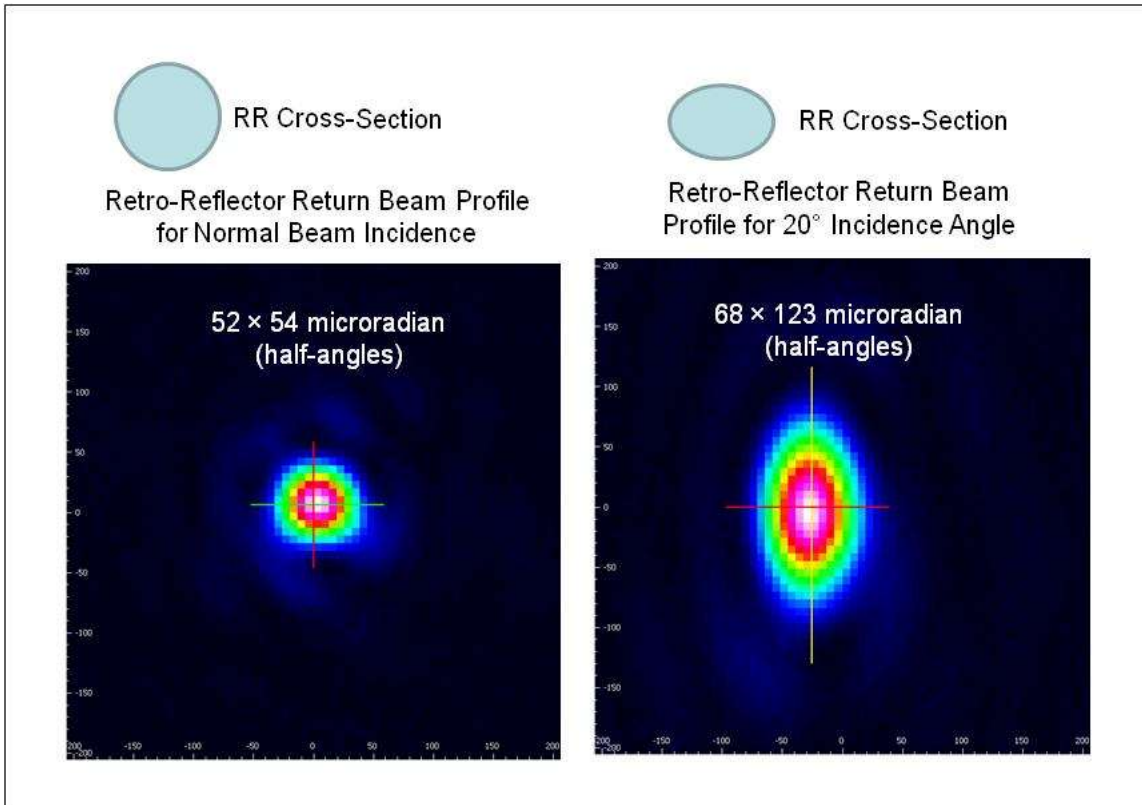
Figure 3 Return Beam Profiles for On-Axis and Oblique (20 deg) Incidence Angles

The other effect impacting the potential utility of the RR for satellite tracking experiments is the decrease in RR cross section as a function of laser incidence angle (defined as zero when on-axis with the RR). Since the STPSAT2 satellite is always NADIR pointing, the laser incidence angle increases with increasing range to the laser site. Figure 4 presents the experimental set-up used to characterize the angular roll-off of the RR using a photodiode to capture the entire return signal as the rotation stage angle is varied. Figure 5 presents the results of this measurement revealing a rapid decrease in relative cross-section as a function of incidence angle and the device ceases to retro-reflect the beam at approximately 30 degrees off the center axis. It was verified that the angular response of the RR was the same at 1.06 microns confirming that the response drop-off is just due to geometric effects and is not wavelength dependent (as expected for the silver coating).

In summary of the RR characterization, the 1.27 cm hollow retroreflector is expected to produce a return beam of sufficient strength to be useable by ILRS sites even given the velocity aberration expected for the specific conditions of the STPSAT2 satellite. The roll-off in response as a function of range to the satellite is expected to be somewhat compensated for by the large beam profile produced when the RR is in oblique geometries.
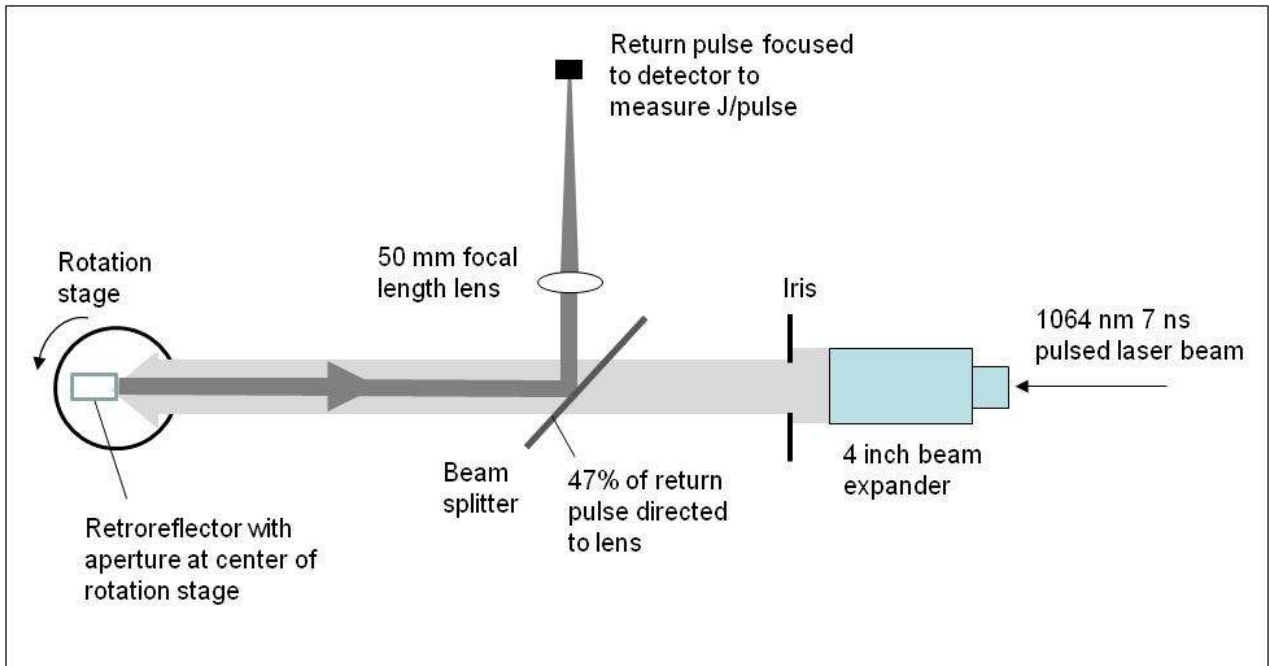
Figure 4. Set-up for Angular Response Retroreflector Measurements
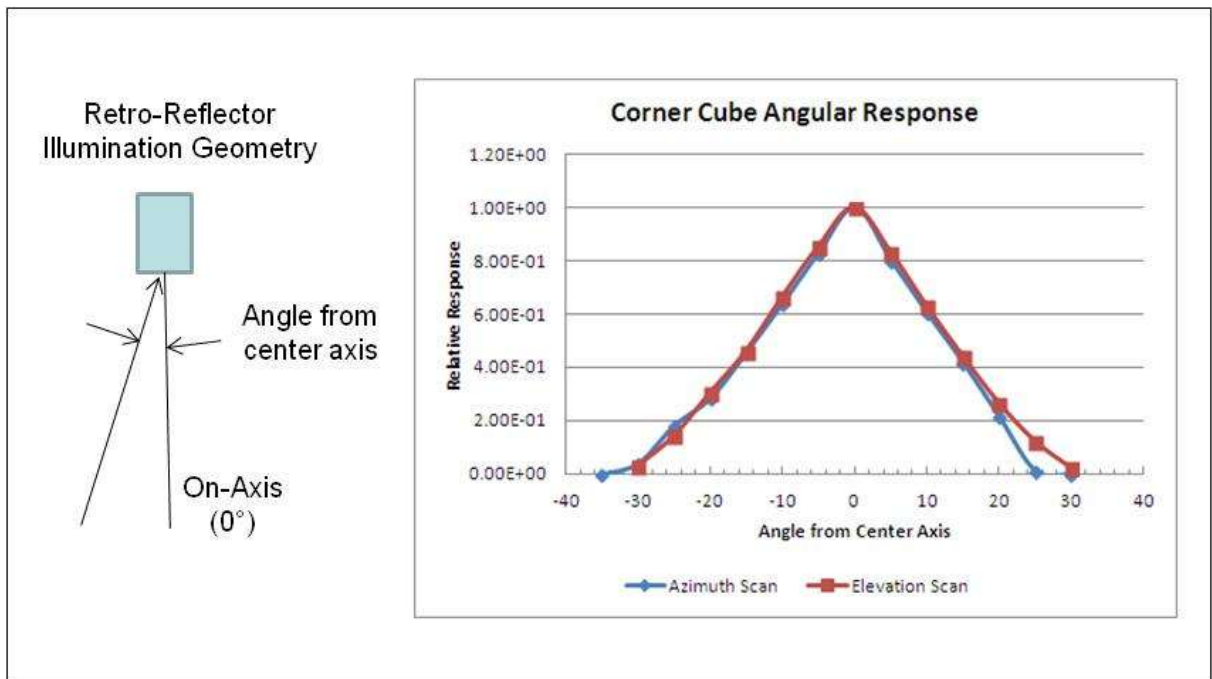
Figure 5. Angular Cross Section Measurement of Retroreflector

3.2 Laser Sites Used in Evaluation

Table 1 presents a summary of the sites that reported testing with the STPSAT-2 satellite.[4] A substantial number of observations were made over the experimental time window. The initial analysis for the RR performance was based on the first few months of the experimental window. At the time of this analysis, the only four sites which reported measured returns are those listed in Table 2. Since the purpose of the analysis was to determine the RR utility, only cases with reported returns were considered. Additional analysis considering a greater number of sources is planned in the future.

Table 1 ILRS Test Summary for STPSAT-2

Station	First Observation	Last Observation	Passes	Observations	Duration in [s]
18248101, Golosiiv	4/12/2013 17:46	12/14/2013 17:42	4	17	331
70900513, Yarragadee	4/2/2013 18:29	9/26/2013 15:34	12	48	786
71050725, Greenbelt	6/21/2013 3:01	8/5/2013 2:52	2	8	100
71100412, Monument Peak	4/27/2013 3:27	9/25/2013 8:59	8	43	644
72371901, Changchun	6/14/2013 14:59	9/27/2013 16:17	9	26	352
74057904, Concepcion	9/17/2013 19:43	9/17/2013 19:44	1	4	55
74068801, San Juan	9/5/2013 5:01	9/25/2014 6:45	374	8462	141258
75010602, Hartebeesthoek	6/6/2013 21:20	6/6/2013 21:20	1	2	16
78106801, Zimmerwald	0000-00-00 00:00:00	0000-00-00 00:00:00	2	5	0
78208201, Kunming	6/13/2013 16:04	6/18/2013 14:51	2	13	842
78212801, Shanghai	7/19/2013 17:30	8/13/2013 2:13	2	8	106
78403501, Herstmonceux	4/20/2013 20:10	9/16/2013 4:00	4	16	302
78418701, Potsdam	4/24/2013 18:25	10/3/2013 23:33	9	61	2087
78457801, Grasse	8/9/2013 20:38	8/9/2013 20:39	1	4	53
79417701, Matera	6/12/2013 22:20	6/12/2013 22:20	1	3	33
88341001, Wettzell	6/13/2013 22:45	6/13/2013 22:46	1	3	25

Table 2. Sites Reporting Return Hits During Initial Period of the STPSAT-2 Retroreflector Characterization

Site	Symbol	Source
Greenbelt, Maryland	GODL	532 nm, 150 ps pulse
Yarragadee, Australia	YARL	532 nm, 150 ps pulse
Hartebeesthoek, South Africa	HARL	532 nm, 150 ps pulse
Monument Peak, California	MONL	532 nm, 150 ps pulse

---

[4] http://edc.dgfi.badw.de/en/satellites/stpsat2/

4.0 Results

Figures 6-13 present selected data from the four different sites that reported return amplitudes during this campaign. Figure 6 is for a pass over the MONL site on 7/254/13 and it was selected for discussion since it was a long pass with nearly continuous returns to the site. The bottom panel of 6 shows the satellite ground track during the pass and the data reported by MONL is displayed as a function of time (top trace), as a function of distance (middle trace) and as a function of incidence angle to the retroreflector (bottom trace, zero being the NADIR direction). Based on equation 5, one expects an amplitude dependence of R^{-4} consistent with a standard propagation range equation. Using the middle trace in Figure 6, the distance change from detection at 665 km to that at 750 km should translate into an amplitude drop of $(665/750)^4$ or a 40% decrease in return signal strength. However, the amplitudes are nearly uniform over that range and actually increase in the 720-730 km range. The uniformity in amplitude response may be partly due to the increase in return beam divergence as a function of range which compensates for the range effect and reduced cross section. Other effects such as beam pointing variations, polarization effects or differences in atmospheric transmission could also impact the received amplitude distribution. However, the loss of signals beyond an incidence angle of 30 degrees shows that the abrupt end of a retro-reflected beam is the primary limitation in the utility of this device for satellite tracking experiments. Similar conclusions can be drawn from the other data from MONL, YARL and GODL as seen in Figures 7-12. The data from HARL, shown in Figure 13, is sparser than the other sites, so the angular response impact is not as evident.
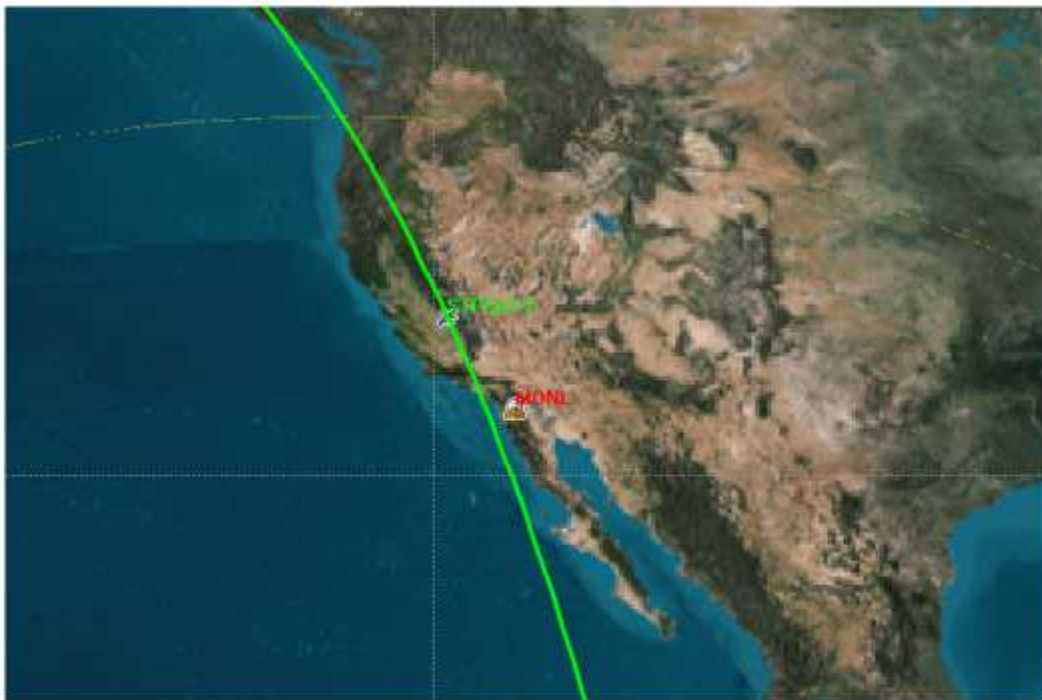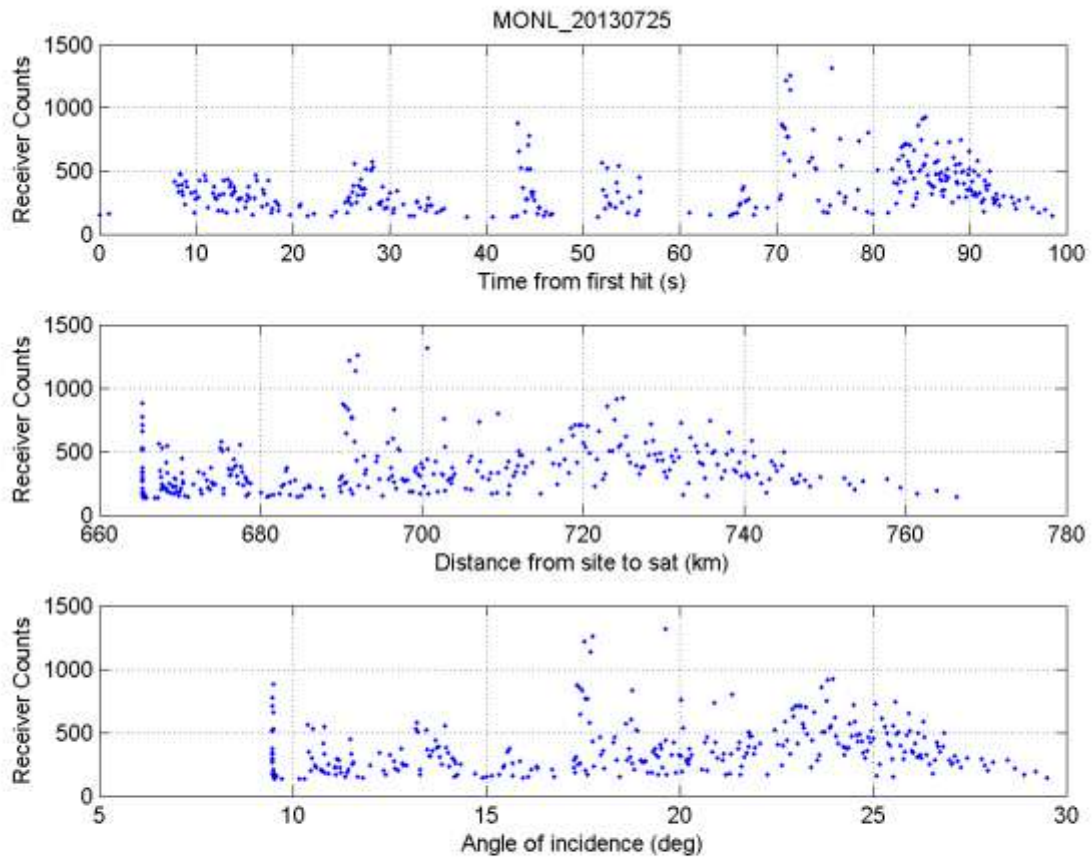
Figure 6. MONL Data from July 25, 2013
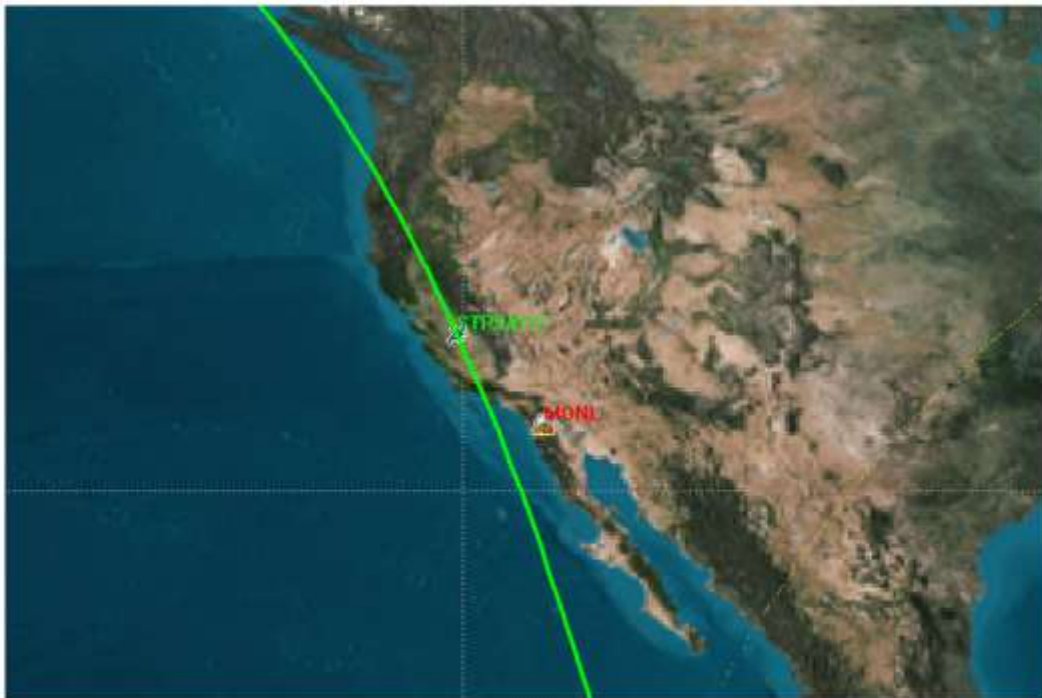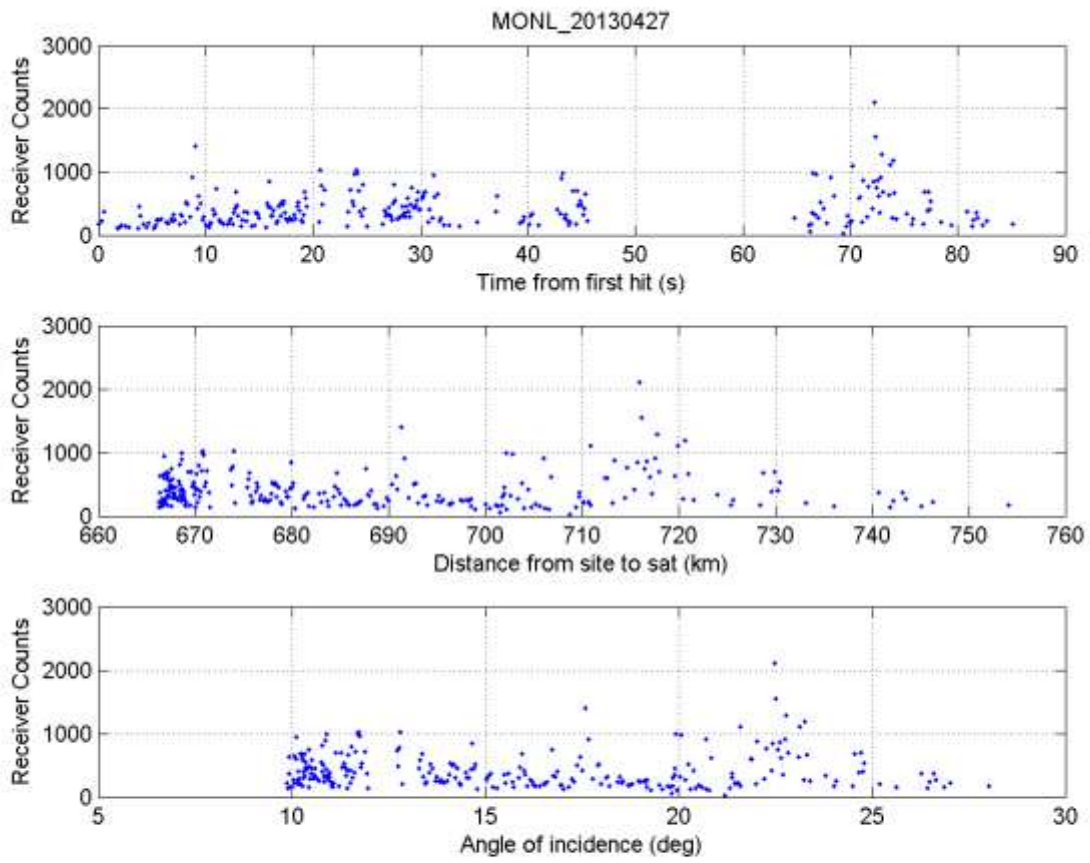
Figure 7. MONL Data from April 25, 2013

10
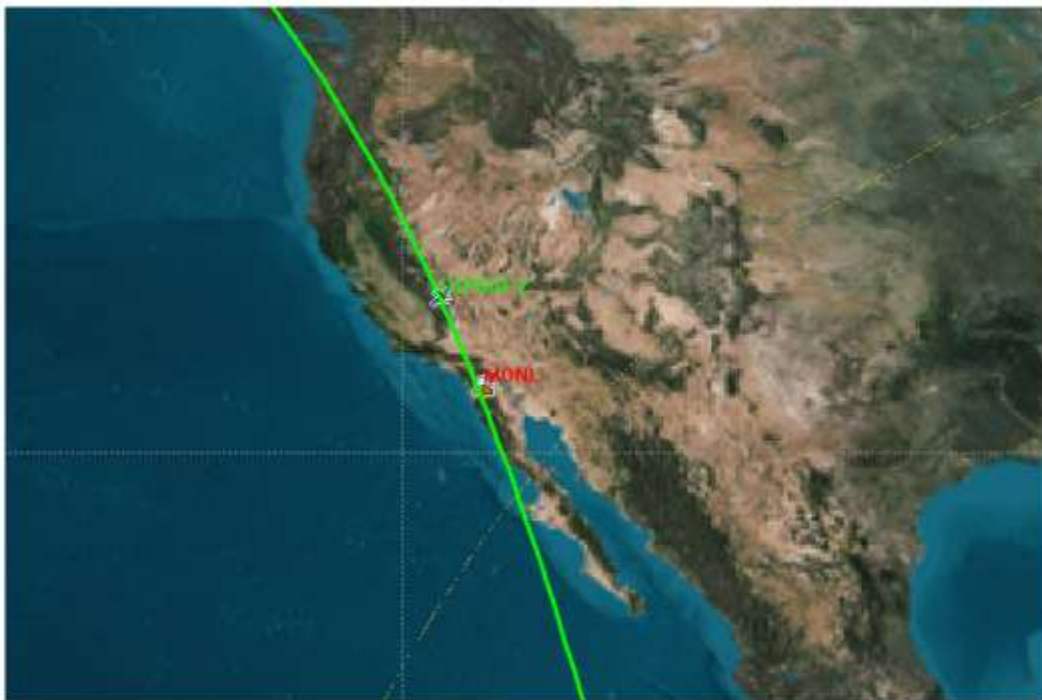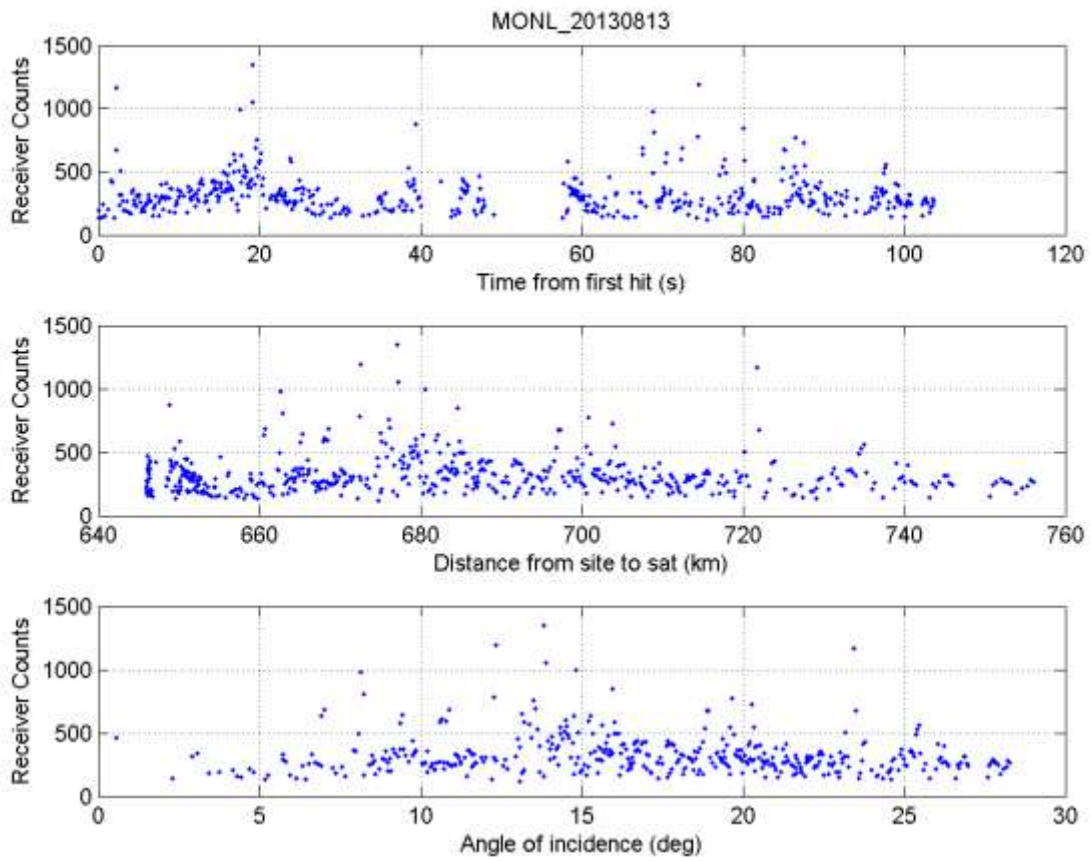
Figure 8. MONL Data from August 13, 2013
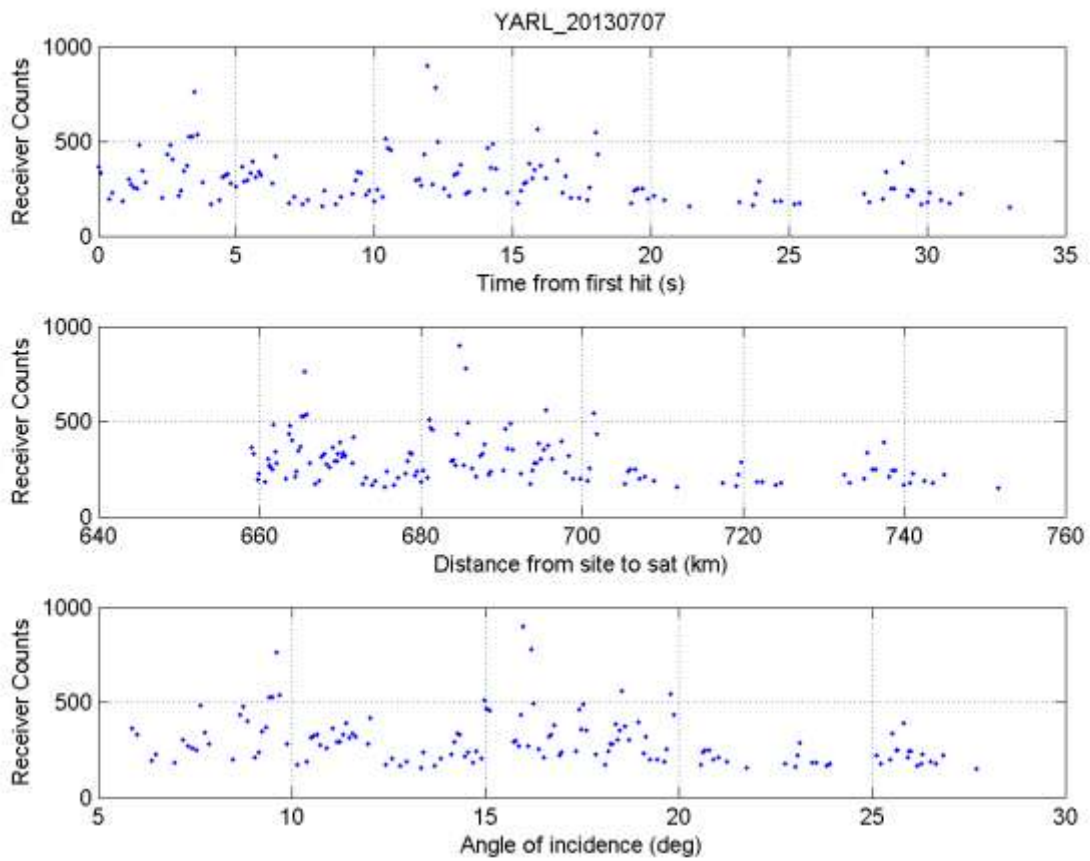
Figure 9. YARL Data from July 7, 2013
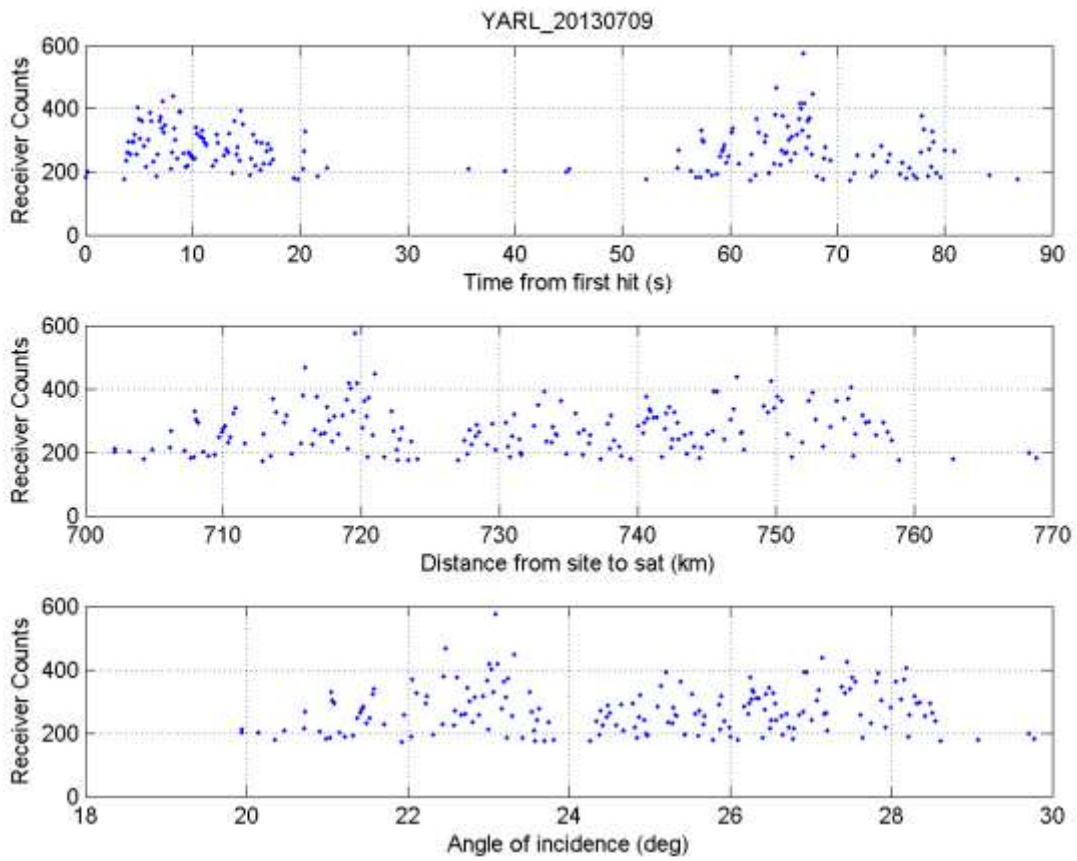
Figure 10. YARL Data from July 9, 2013
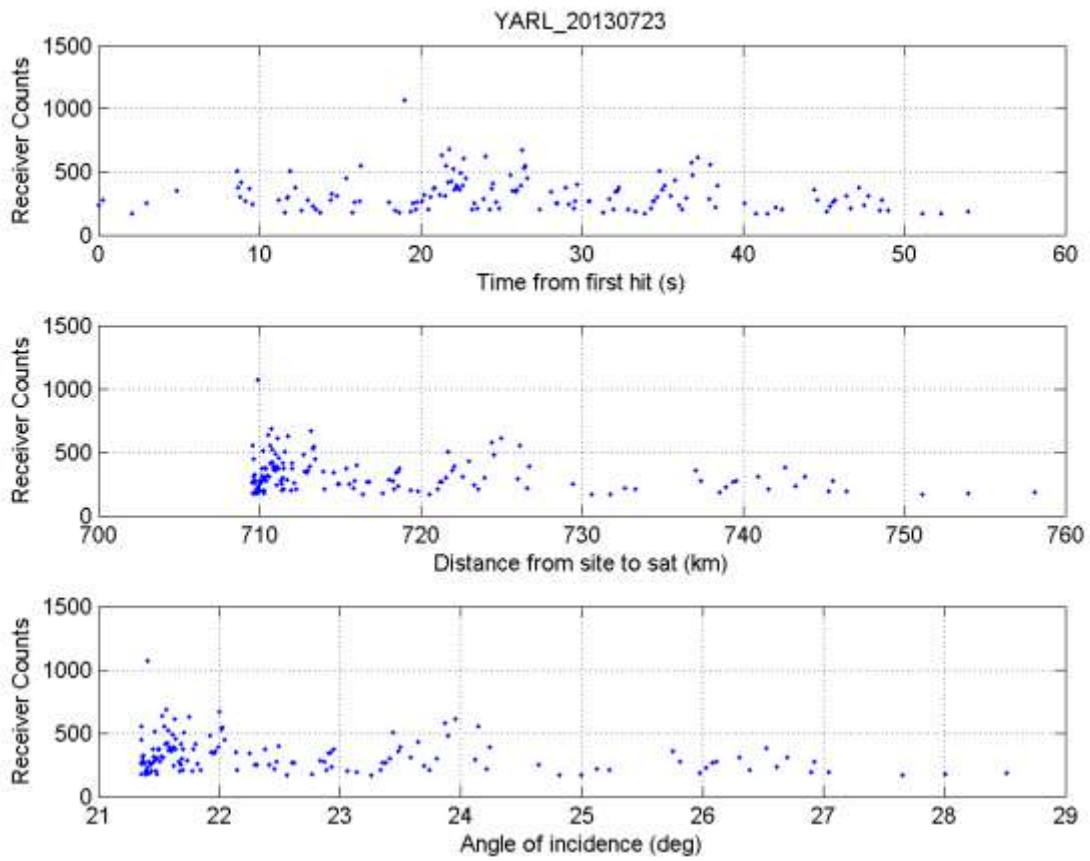
Figure 11. YARL Data from July 23, 2013
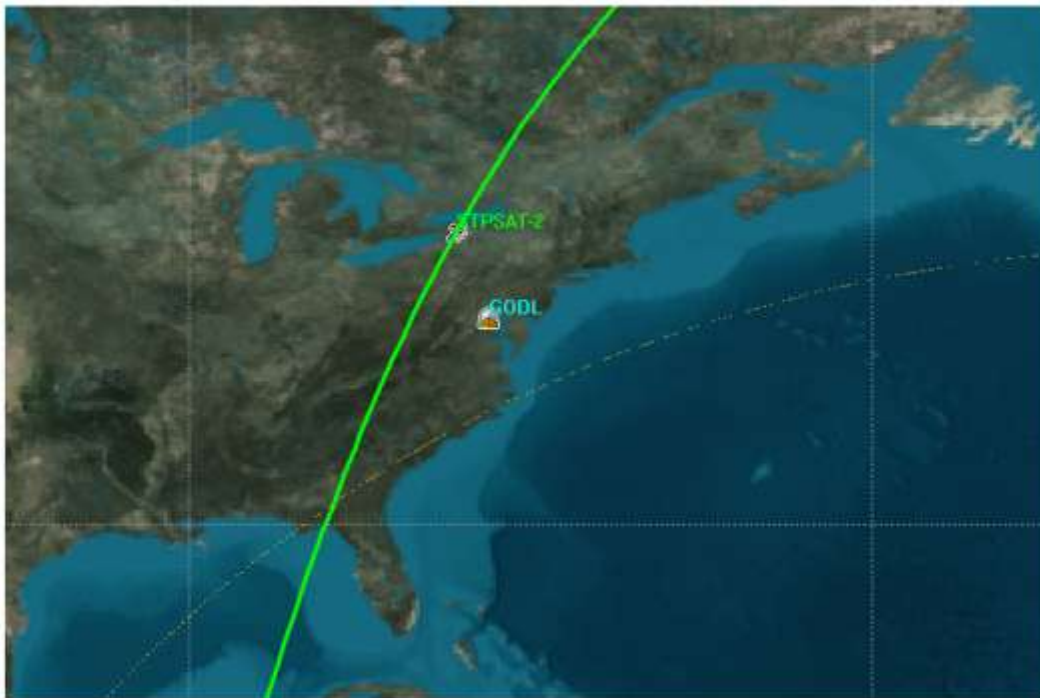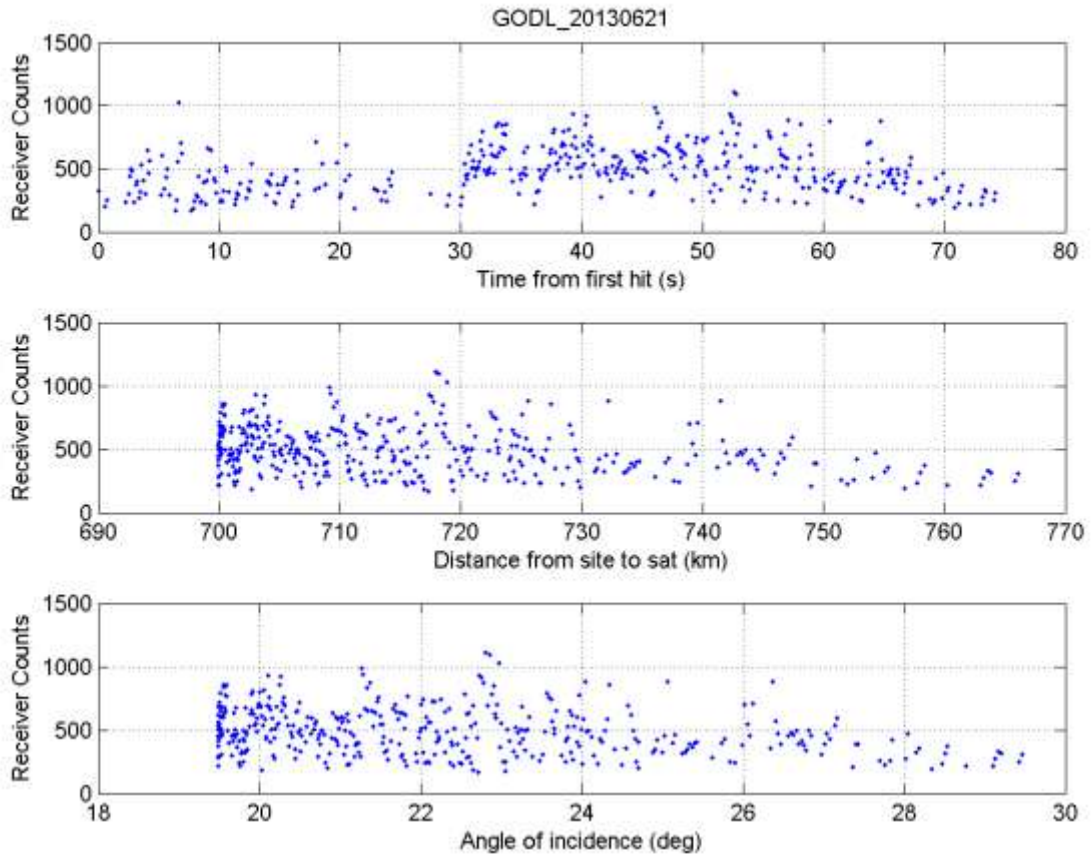
Figure 12. GODL Data from June 21, 2013

15
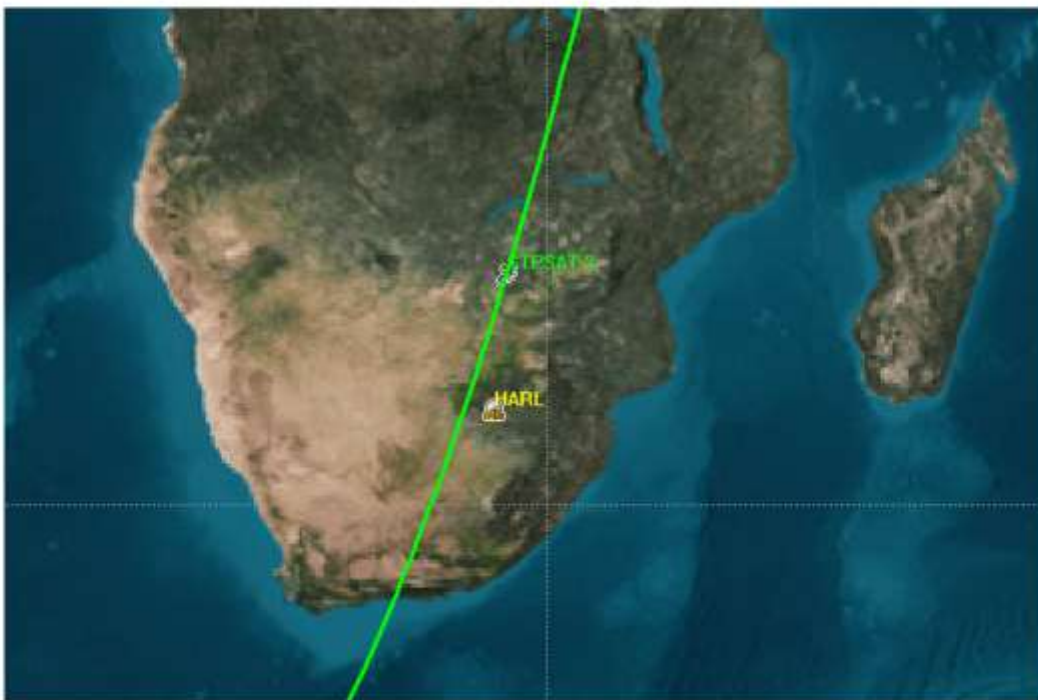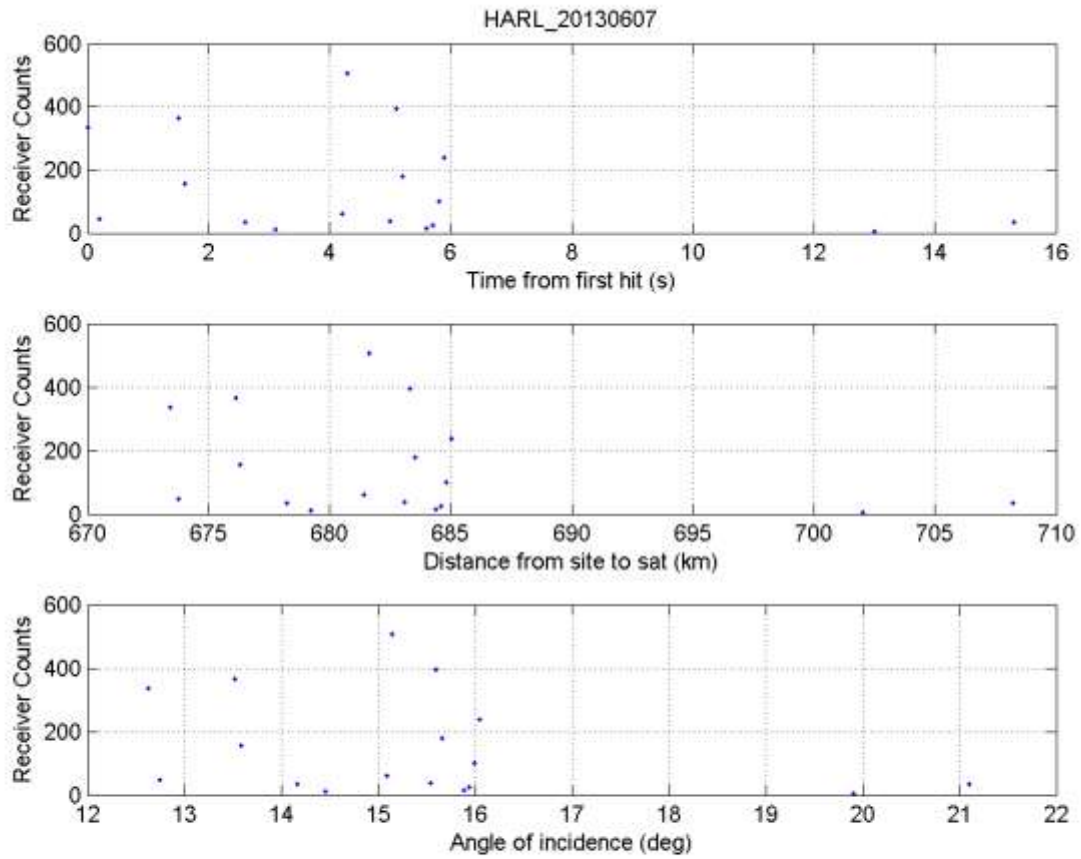
Figure 13. HARL Data from June 7, 2013

5.0 Conclusions and Future Experiments

A successful experimental campaign was carried out with the ½ inch hollow retroreflector on the STPSAT-2 satellite verifying its utility for supporting tracking studies with ILRS-class lasers. An advantage of using a hollow retro-reflector rather than glass-filled is that it can be used with a larger range of laser wavelengths and the STPSAT-2 experiments showed that the hollow device survived launch and was functioning properly after 2.5 years on-orbit.

The tests carried out also verified that the angular response of the device in a NADIR facing orientation is what limits the angles and distances over which it can produce useful returns for tracking experiments. For experiments at 1.06 microns, the 1.27 cm device is suitable given that the return beam divergence is greater than the velocity aberration. Having the device on a small satellite that can be pointed will greatly expand its utility for tracking experiments. However, depending on the satellite altitude and laser wavelengths used, the retroreflector dihedral angles and diameter may need to be tailored to optimize the optical cross section for the velocity aberration expected.